Wavelength-encoding/temporal-spreading optical code division multiple-access system with in-fiber chirped moiré gratings

Lawrence R. Chen, Peter W. E. Smith, and C. Martijn de Sterke

We propose an optical code division multiple-access (OCDMA) system that uses in-fiber chirped moiré gratings (CMG's) for encoding and decoding of broadband pulses. In reflection the wavelength-selective and dispersive nature of CMG's can be used to implement wavelength-encoding/temporal-spreading OCDMA. We give examples of codes designed around the constraints imposed by the encoding devices and present numerical simulations that demonstrate the proposed concept. © 1999 Optical Society of America

OCIS codes: 060.2330, 050.2770.

1. Introduction

Optical code division multiple-access (OCDMA) is of interest as a multiaccess technique in local area networks, since it potentially allows many users to share a single transmission medium asynchronously. Among its other attractive characteristics are the potential for increased security, high capacity, and less stringent wavelength control compared with wavelength-division-multiplexed systems.[1,2] Bits of information are transmitted with optical pulses: a 1 (0) bit is represented by the presence (absence) of an optical pulse. The signals transmitted by different users, which are broadcast simultaneously to all the receivers in the network, are encoded into different wave forms, or code sequences, which represent address information. At the receivers a matched filter or decoder is used to ensure that data are detected only when they have arrived at the proper destination. Multiple access is achieved by assignment of minimally interfering codes to each user pair.

Recently there have been several proposals for using in-fiber Bragg gratings to implement OCDMA. For example, cascaded and binary-sampled gratings have been used in frequency-hopping and direct-sequence CDMA schemes.[3–7] In this paper we show how in-fiber chirped moiré gratings (CMG's) can also be used as encoding and decoding elements to implement wavelength-encoding/temporal-spreading OCDMA. Our proposed scheme differs from other wavelength-hopping/temporal-spreading implementations[6–8] in that no rapidly tunable source is required for providing the wavelength encoding (the wavelengths are instead provided by a broadband input), and only a single grating structure (rather than cascaded gratings) is needed for encoding and decoding.

This paper is organized as follows. In Section 2 we qualitatively describe how CMG's can be used to encode and decode optical pulses and provide a numerical simulation example that demonstrates the concept. In Section 3 we present the design of suitable codes that take into account the constraints imposed by the CMG encoding devices and numerically evaluate the performance of the system in terms of the probability of error. In Section 4 we discuss the various practical issues that are relevant to our proposed system, and finally in Section 5 we summarize our results and conclude.

L. R. Chen and P. W. E. Smith are with the Department of Electrical and Computer Engineering, University of Toronto and Photonics Research Ontario, 10 King's College Road, Toronto, Ontario, M5S 3G4 Canada. C. M. de Sterke is with the School of Physics, The University of Sydney, New South Wales 2006, Australia, and the Australian Photonics Cooperative Research Centre, Australian Technology Park, New South Wales 1430, Australia. The e-mail address for L. R. Chen is chenl@ecf.utoronto.ca.

Received 12 January 1999; revised manuscript received 26 March 1999.

0003-6935/99/214500-09$15.00/0

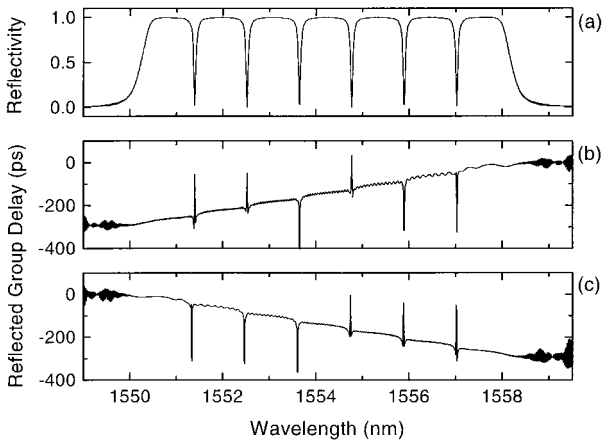

Fig. 1. (a) Reflection response of a 3-cm-long CMG with $\delta n = 8.0 \times 10^{-4}$, $\lambda_1 = 2n_0\Lambda_1{}^0 = 1550.0$ nm, $\lambda_2 = 2n_0\Lambda_2{}^0 = 1550.2$ nm, and equal chirp parameters for both gratings $\delta\Lambda_1 = \delta\Lambda_2 = d\Lambda = 5.0 \times 10^{-14}$ nm^2/m; (b) corresponding reflected group delay of the CMG and (c) its physically reversed structure. The spikes in the group delay occur where the phase of the reflection coefficient changes by π.

2. Chirped Moiré Gratings for Encoding and Decoding

A. Qualitative Description

A CMG consists of two superimposed linearly chirped Bragg gratings.[9–11] The refractive-index modulation that represents the grating can be written as[10]

$$n(z) = n_0 + \delta n \cos\left(\frac{2\pi z}{\Lambda_1}\right) + \delta n \cos\left(\frac{2\pi z}{\Lambda_2}\right) = n_0 + \Delta n(z)\cos\left(\frac{2\pi z}{\Lambda_s}\right),$$

where n_0 is the average refractive index of the unmodified fiber; δn is the peak refractive index modulation; $\Delta n(z) = \delta n \cos(2\pi z/\Lambda_c)$; $\Lambda_c = 2[|1/\Lambda_1 - 1/\Lambda_2|]^{-1}$ and $\Lambda_s = 2[1/\Lambda_1 + 1/\Lambda_2]^{-1}$ are the period of the slowly varying envelope and the rapidly varying component of the grating, respectively; and Λ_1 and Λ_2 are the periods of the superimposed gratings, each varying linearly as a function of position: $\Lambda_i = \Lambda_i{}^0 + (\delta\Lambda_i/\Lambda_i{}^0)z$, $i = 1, 2$. There are crossover points of the beat in the grating fringe pattern where the phase of the grating changes by π, with each producing a passband in the transmission response.[11] The multiple passbands can also be interpreted as Fabry–Perot resonances of the two mirrors formed by the two superimposed gratings.[10] Obviously, these passbands have the effect of creating spectrally separated stop bands in reflection.

Figure 1(a) shows the calculated spectral response of a 3-cm-long CMG with $\delta n = 8.0 \times 10^{-4}$, $\lambda_1 = 2n_0\Lambda_1{}^0 = 1550.0$ nm, $\lambda_2 = 2n_0\Lambda_2{}^0 = 1550.2$ nm, and equal chirp parameters for both gratings $\delta\Lambda_1 = \delta\Lambda_2 = 5.0 \times 10^{-14}$ nm^2/m. This CMG has seven reflection stop bands. Of greater interest is the corresponding reflected group delay, shown in Fig. 1(b). Since the relationship between reflected wavelengths and time is linear (owing to the linear chirp in the gratings), each stop band is reflected in its own time slot. A CMG in reflection can then be used to decompose a short broadband (input) pulse simultaneously in both wavelength and time domains; its functionality is similar to that of cascaded gratings in terms of encoding operations.[3,4,6] The physically reversed CMG structure has the same reflectivity (spectral response).[4,12] The reversed grating structure also has, to first order, opposite reflected group delay as shown in Fig. 1(c) (this principle has been demonstrated[13] in an experiment in which pulses were broadened and recompressed by bidirectional reflection from a linearly chirped in-fiber Bragg grating). We can thus envision encoding and decoding broadband pulses by successive reflections from a CMG (encoding) and its physically reversed structure (decoding).

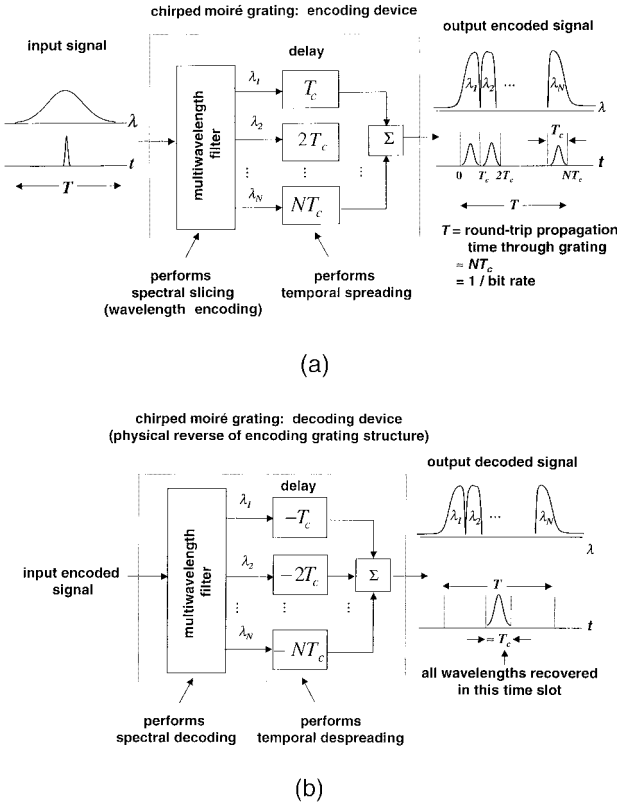

Fig. 2. Schematic illustration of (a) encoding and (b) decoding an ultrashort broadband pulse with CMG's. The CMG is modeled as a multiwavelength filter (or discrete set of wavelength filters) with corresponding time delay lines for each filtered wavelength component. The corresponding code illustrated is $c = [1, 2, \ldots, N]$. Different users (codes) would be defined by different spectral slicing patterns (i.e., different wavelength filters) and their corresponding time delay patterns.

A CMG can be modeled as a multiwavelength filter, or as a set of $w \leq N$ discrete wavelength filters, with corresponding time delay lines for each filtered wavelength component (w and N are defined in the next paragraph). It serves two functions in the encoding and decoding processes as illustrated in Fig. 2. First, by selectively filtering wavelength components of the input pulse (i.e., spectral slicing), it performs

wavelength encoding, and second, by temporally arranging these spectral components in a linear fashion, it performs temporal spreading. If the decoder is the physically reversed structure of the encoder, then the filtering operations are identical and the temporal arrangements of the wavelength components are complementary so that proper decoding can be achieved. To perform proper decoding, the decoder must recover all of the wavelengths of the encoded signal into the same time slot, i.e., despread the signal. Note that the original input pulse will not be fully reconstructed, since we performed spectral slicing (i.e., eliminated spectral contents from the pulse). However, properly and improperly decoded signals can be distinguished on the basis of peak intensities, especially within the time slot where all of the wavelengths of the properly decoded signal are recovered.

A given CMG has N spectrally separate reflection stop bands centered at λ_i ($i = 1, \ldots, N$), which occupy N time slots (or chips), each with a duration $T_c \approx T/N$ where T is the round-trip propagation time through the CMG (and would correspond to the bit window). The physical structure and response (spectral and temporal) of a CMG define a corresponding code; thus the code has a length equal to N. A convenient representation of the available codes is a $1 \times N$ array, denoted $c_j = [c_j^1, c_j^2, \ldots, c_j^N]$, where the index of the array defines the time slot (for example, c_j^1 corresponds to time slot 1, and so on) and the values of the $c_j^1, c_j^2, \ldots, c_j^N$ elements represent the central wavelengths in these time slots. Since the wavelengths are reflected sequentially in time, because of the linear relationship between reflected wavelengths and time, a CMG, such as that described in Fig. 1, defines only one code with a weight $w = N$, where the weight corresponds to the number of pulses in the coded wave form (and equivalently, to the number of wavelengths or spectral slices). It is possible to modify the spectral response of a CMG to choose only q of the available N reflection stop bands (wavelengths) for one code so that $w = q < N$. We can accomplish this by selectively eliminating stop bands from the CMG response by incorporating regions within the grating structure where there is no refractive-index modulation.[14,15] Essentially, we are defining different spectral slicing (wavelength-encoding) patterns that would correspond to different codes. The code length is still N as defined by the number of time slots that correspond to the original CMG; however, $N - w$ of the entries in the code are 0 (no signal), and the w nonzero entries correspond to the wavelengths of retained stop bands. We can then define a maximum of $\tilde{m} = \lfloor N/q \rfloor = \lfloor N/w \rfloor$ codes that are strictly orthogonal (i.e., the codes have no spectral overlap), where $\lfloor \bullet \rfloor$ denotes the integer part of the argument. To generate additional codes, the strictly orthogonal codes that we define can be simply wavelength shifted. These new codes are only quasi orthogonal, since there may be some spectral overlap between the shifted and the original codes. In the above, strictly orthogonal codes refer to those that are strictly noninterfering (the codes have a cross correlation that is identically 0) and quasi-orthogonal codes are those that are minimally interfering (the codes have specific cross-correlation properties that are defined in Subsection 3.B).

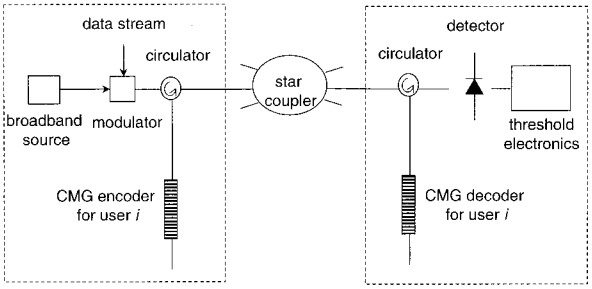

Fig. 3. Implementation of CMG encoders–decoders in an OCDMA system.

B. Implementation of Chirped Moiré Grating Encoders–Decoders in an Optical Code Division Multiple-Access System

Figure 3 illustrates one possible implementation of an OCDMA network which uses CMG's as encoders–decoders. Each transmitter comprises a broadband source (mode-locked laser, gain-switched laser diode, amplified spontaneous emission from an erbium-doped fiber amplifier, and so on), a modulator, and a CMG encoder; each receiver comprises a CMG decoder and a detection unit (photodiode, threshold electronics, and so on). A given user pair i communicates over the network as follows. The data string is modulated onto the output of the broadband source, giving a string of pulses (bits) that are then reflected from the CMG encoder. The encoded signal is then broadcast to all receivers in the network by means of a star coupler. Following the decoding and the threshold detection processes, only the desired receiver that has the proper CMG decoder (i.e., the physically reversed structure of the CMG encoder) will be able to recover the information sent. Note that all the encoding and decoding operations are performed in-fiber.

C. Numerical Example

We now consider a concrete example that illustrates encoding and both proper and improper decoding processes. Let $N = 7$ and $w = 3$. We can define at most two strictly orthogonal codes, for example, $c_1 = [0,2,3,0,0,6,0]$ and $c_2 = [1,0,0,4,0,0,7]$. We can also define quasi-orthogonal codes that are wavelength-shifted versions of c_1 and c_2, one of which is $c_3 = [0,1,2,0,0,5,0]$. The encoded and the decoded wave forms for a user with code c_j are denoted as $c_j^{\mathrm{enc}}(t)$ and $c_j^{\mathrm{dec}}(t)$, respectively. Figure 4(a) shows the spectral responses of three CMG's that generate the three codes c_1, c_2, and c_3 (in the codes, λ_1 corresponds to the stop band centered at $\approx$1550.9 nm, and so on). These three CMG's have the same parameters (length, peak index modulation, difference in central periods or wavelengths of the two superimposed grat-

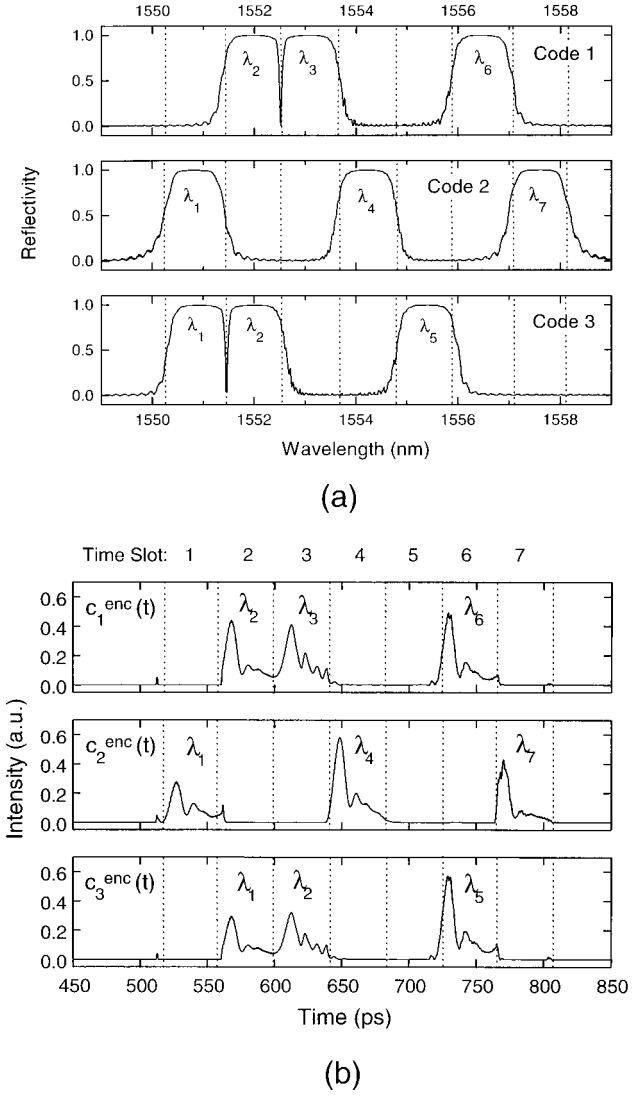

Fig. 4. Simulation of encoding a 0.5-ps transform-limited Gaussian pulse. (a) Spectral response of the CMG's that correspond to the three codes outlined in the text and (b) corresponding encoded wave forms. The dotted lines show the time slots (chips).

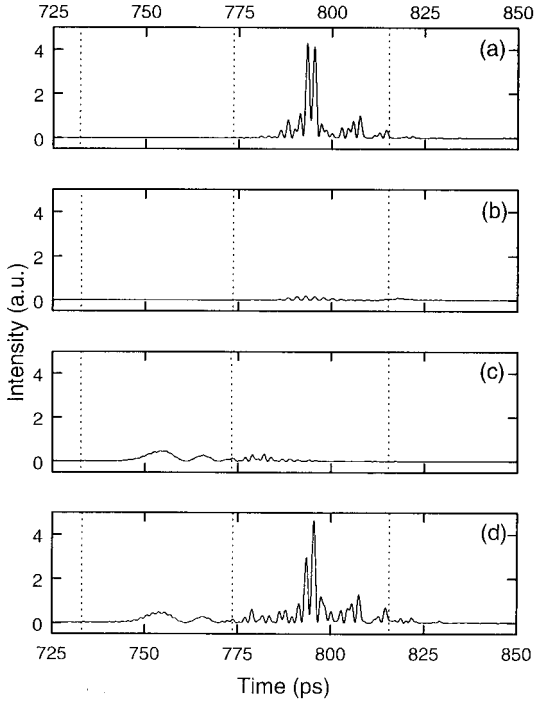

Fig. 5. Simulation of proper and improper decoding of encoded wave forms in Fig. 4(b). Decoded wave forms: (a) $c_1^{dec}(t)$, (b) $c_2^{dec}(t)$, and (c) $c_3^{dec}(t)$; (d) the decoded wave form of $c_1^{enc}(t) + c_2^{enc}(t) + c_3^{enc}(t)$. Note the similarity with $c_1^{dec}(t)$; additional multiuser interference can be suppressed by means of time gating. All decoding was performed with the decoder for code c_1. The dotted lines show the time slots (chips).

ings) as in Fig. 1 except that they incorporate regions of no refractive-index modulation within the grating structure to obtain the desired spectral response by suppressing selected stop bands. Specifically, the CMG for c_1 has three regions of lengths 0.5, 1.0, and 0.5 cm centered at $z = 0.25$, 1.75, and 2.75 cm, respectively, where there is no index modulation; the CMG for c_2 has two regions of equal length, 0.75 cm centered at $z = 0.875$ and 2.125 cm where there is no index modulation; and the CMG for c_3 is identical to that for c_1 except for different grating periods that shift the wavelengths. Figure 4(b) shows the wave forms that correspond to the different codes, assuming a transform-limited 0.5-ps Gaussian pulse at $\lambda = 1554.25$ nm as the input. Note that codes c_1 and c_3 have the same time-spreading pattern but different wavelength-encoding patterns. Thus the encoded signals $c_1^{enc}(t)$ and $c_3^{enc}(t)$ will have pulses in the same time slots, but the pulses will be at different wavelengths.

Figures 5(a)–5(c) show the result of decoding $c_1^{enc}(t)$, $c_2^{enc}(t)$, and $c_3^{enc}(t)$ with the decoder for code c_1. As expected, $c_1^{dec}(t)$ has the largest signal, owing to proper decoding, whereas $c_2^{dec}(t) \approx 0$, owing to the orthogonality of c_1 and c_2. Although there is some spectral overlap between the CMG's that define c_1 and c_2 [see Fig. 4(a)] so that strictly $c_2^{dec}(t) \neq 0$, the energy of $c_1^{dec}(t)$ is clearly much greater than that of $c_2^{dec}(t)$. Also, codes c_1 and c_3 have one overlapping stop band at $\lambda_2 \approx 1552$ nm so that part of $c_3^{enc}(t)$ will be decoded by the decoder for code c_1. However, its wavelength–time relationship is such that the overlapping stop band will be recovered into a different time slot than that for the stop bands in $c_1^{enc}(t)$, as can be seen by examination of the wavelength–time relationships given by the codes. Thus the properly decoded signal $c_1^{dec}(t)$ will have all of its wavelength components recovered into a different time slot from that of an improperly decoded signal, e.g., $c_3^{dec}(t)$. In fact, they will be separated in time by at least T_c, the duration of a reflection stop band. Properly and improperly decoded signals can be further distinguished by use of time gating (which selects the time slot within the bit window when the detector samples the decoded signal) to suppress undesired signals. We also consider decoding the input signal $c_1^{enc}(t) + c_2^{enc}(t) + c_3^{enc}(t)$ with the decoder for code c_1. As shown in

Fig. 5(d), the desired signal $c_1^{dec}(t)$ can still be recovered even in the presence of undesired signals from c_2 and c_3 by use of the appropriate decoder. Note that similar results will be obtained if any incoherent pulsed broadband source (rather than the transform-limited pulse) is used, except that there will be a decrease in the peak of the signals, since the energy will be more spread in the time slots (because there is no coherent interference).

The number of codes (users) that can be supported is determined primarily by the value of N and can vary from 1 to greater than N. Furthermore, we can design L and N such that $T_c = T/N = (2Ln_0)/(Nc)$, where c is the speed of light, will be sufficiently long to allow for the time gating to be performed electronically. We have more to say about the use of time gating in Section 4.

3. Code Design and Performance

A. Design

Assume that the N reflection stop bands of a given CMG occupy the range $[\lambda_{min}, \lambda_{max}]$, which spans the entire bandwidth (BW) of the broadband input pulse, i.e., $[\lambda_{min}, \lambda_{max}] = [\lambda_{min}^{pulse}, \lambda_{max}^{pulse}]$. In the following notation the wavelengths represent the central wavelengths of the stop bands. We can then write $\lambda_{max} = \lambda_{min} + (N - 1)\Delta\lambda$, where $\Delta\lambda$ is the BW of a stop band. If we measure wavelength in units of $\Delta\lambda$ so that in these normalized units $\Delta\lambda = 1$, then $\lambda_{max} = \lambda_{min} + (N - 1)$. As mentioned earlier, we can choose to define m ($\leq \tilde{m} = \lfloor N/w \rfloor$) codes that use only w of the available N stop bands, (i.e., a code of length N with a weight of w). These strictly orthogonal codes define m temporal-spreading patterns coupled to m wavelength-encoding patterns. We refer to them as the original m codes. Note that the combined wavelength-selective and dispersive natures of the CMG's are responsible for coupling the temporal-spreading and the wavelength-encoding patterns. They are not independent.

Additional codes can be obtained by wavelength-shifting of the original m codes: All the wavelengths in each of the m time-spreading patterns are simply shifted by $n\Delta\lambda = n$, an integer multiple of the BW of a stop band. This can be accomplished physically by strain or compression tuning of the m CMG structures that correspond to the original m codes. Since we have assumed that the N stop bands span the entire pulse BW, the new wavelengths in the shifted codes must still lie in the range $[\lambda_{min}, \lambda_{max}]$. Let the w wavelengths for a given code c_j occupy $[\lambda_{min}^j, \lambda_{max}^j]$. This code allows for lower and upper wavelength shifts of $(\lambda_{min}^j - \lambda_{min})$ and $(\lambda_{max} - \lambda_{max}^j)$, respectively. From the time-spreading pattern corresponding to c_j, there are then a total of $N - (\lambda_{max}^j - \lambda_{min}^j)$ wavelength-encoding patterns, all with the same time-spreading pattern, that can be generated. Thus, from a given N, w, and set of original m time-spreading patterns, we can obtain the following maximum number of codes:

$$Nm - \left(\sum_{j=1}^{m} [\lambda_{max}^j - \lambda_{min}^j] \right). \tag{1}$$

We now need to specify the original m time-spreading patterns (or codes). Simple combinatorial analysis shows that there are a total of

$$\sum_{k=0}^{m-1} (N - kw|w) = \sum_{k=0}^{m-1} \frac{(N - kw)!}{w![N - (k + 1)w]!} \tag{2}$$

from which to choose these m codes.[16] Multiuser interference is controlled by the cross correlation of the code sequences. To minimize the interference, the codes should have a maximum (Hamming) cross-correlation peak (defined in Subsection 3.B) equal to 1 (so-called one-coincidence sequences)[17]; thus certain restrictions on the initial choices need to be imposed. Since the original m codes are strictly orthogonal, the restrictions are made to affect their wavelength-shifted versions. First, we do not want a wavelength-shifted version of one of the original m codes to coincide with (i.e., have wavelengths identical to) another of the original codes. Thus no two of the original codes can have similar time-spreading patterns. For example, the two codes c_1 = [0,2,0,4,0,0,7,0,0] and c_2 = [1,0,3,0,0,6,0,0,0] will result in a wavelength-shifted version of one code that coincides with the other. Second, for any two of the original m codes, the same number of time slots (chips) cannot separate any two wavelengths in their respective codes, unless the amount of shift necessary to make a wavelength-shifted code have a cross-correlation peak of >1 exceeds the maximum allowed lower or upper shifts. For example, consider the two codes c_1 = [0,2,0,0,5,0,7,0,0] and c_2 = [1,0,0,4,0,0,0,9]. Wavelengths λ_2 and λ_5 in c_1 and λ_1 and λ_4 in c_2 are separated by the three time slots; thus a wavelength-shifted version of c_1, specifically c_1^{shift} = [0,1,0,0,4,0,6,0,0], and c_2 will have a cross-correlation peak of 2. However, the two codes c_1 = [1,0,0,4,0,6,0,0,0] and c_2 = [0,0,3,0,5,0,0,0,9] cannot be wavelength shifted to give a cross-correlation peak of >1, even though wavelengths λ_4 and λ_6 in c_1 and λ_3 and λ_5 in c_2 are separated by the same number of time slots (=2). Note that the first requirement is inherently contained in the second. Clearly then, the number of available codes from which the original m codes can be chosen is less than that given in Eq. (2). We propose the following algorithm to choose the original m codes:

1. Choose a code c_j from at most $(N - kw|w)$ possible codes ($k = j - 1$).
2. Eliminate from the remaining possible codes those with a single wavelength already used in existing codes $c_1, c_2, \ldots, c_j$.
3. Eliminate from the remaining possible codes those with similar time-spreading patterns or the same number of time slots between consecutive

wavelengths (unless wavelength shifting cannot produce a cross correlation of >1) as in the existing codes $c_1, c_2, \ldots, c_j$.

4. Repeat the above until there are no remaining codes.

The choice of the codes is not unique, and in some cases the maximum number $\tilde{m} = \lfloor N/w \rfloor$ cannot be achieved, i.e., $m < \tilde{m}$. However, the generated codes, in addition to their wavelength-shifted versions, will satisfy the properties of (i) a single autocorrelation peak (no sidelobes) and (ii) a maximum cross-correlation peak of 1.

B. Performance

We now consider a matched-filter receiver and analyze the system performance in terms of multiuser interference (but neglecting all other sources of noise) as a function of the number of simultaneous users (K). The following analysis is only approximate and is based on the following assumptions: (1) perfect time slot (chip) synchronization between all interfering users, (2) ideal rectangular-shaped temporal pulses and spectral slices for the encoded and the decoded signals, (3) incoherent superposition of multiuser interference (a pulsed broadband source is used as the input to the encoders), (4) a Gaussian distribution for multiuser interference, and (5) the variance of multiuser interference, σ^2, is approximated by the variance of the amplitude of the cross correlation of $(K - 1)$ uncorrelated users,[6]

$$\sigma^2 = (K - 1)\bar{\sigma}_{i,j}{}^2, \tag{3}$$

where $\bar{\sigma}_{i,j}{}^2$ is the average value of the variance of the cross correlation between pairs of codes c_i and c_j given in terms of the Hamming cross correlation[17]:

$$\sigma_{i,j}{}^2 = \frac{1}{N}\sum_{\tau=0}^{N-1}[H_{i,j}(\tau) - \bar{H}_{i,j}{}^2],$$

where

$$H_{i,j}(\tau) = \sum_{s=1}^{N} h[c_i(s), c_j(s + \tau)], \qquad 0 \le \tau \le N,$$

with

(i) $h(a, b) = \begin{cases} 0, & a \neq b \\ 1, & a = b \end{cases}$;

(ii) $(s + \tau)$ is taken modulo N;

(iii) $c_i = [c_i{}^1, c_i{}^2, \ldots, c_i{}^N]$ and $c_j = [c_j{}^1, c_j{}^2, \ldots, c_j{}^N]$ are two codes of length N.

With the above assumptions and with the optimum detection threshold $\gamma = w/2 + \mu$, where μ is the average value of the multiuser interference with corresponding variance σ^2 given in Eq. (3), the signal-to-interference ratio (SIR) and probability of error P_{error} are

$$\text{SIR} = \frac{w^2}{\sigma^2} = \frac{w^2}{(K - 1)\bar{\sigma}_{i,j}{}^2}, \tag{4}$$

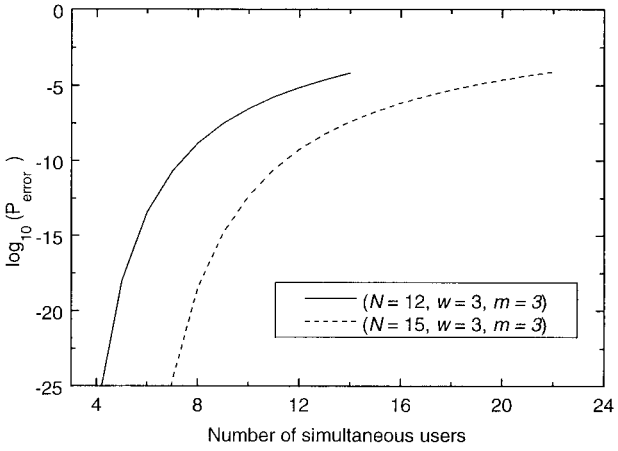

Fig. 6. P_{error} as a function of number simultaneous users.

$$P_{\text{error}} = Q(\sqrt{\text{SIR}}), \tag{5}$$

respectively, where

$$Q(x) = \frac{1}{\sqrt{2\pi}}\int_x^\infty \mathrm{d}t\, \exp\left(-\frac{t^2}{2}\right).$$

Figure 6 shows P_{error}, calculated with Eqs. (3)–(5), as a function of the number of simultaneous users for two cases: $(N = 12, w = 3, m = 3)$ and $(N = 15, w = 3, m = 3)$. The corresponding original m codes and the maximum number of available codes [obtained with Eq. (1)] for each case are given in Table 1 (recall that, once the original m codes are specified, all the codes can be defined). The trends in the results are similar, even when the original m codes are changed, and, in particular, we observe the following. For a fixed w and m, increasing N obviously results in a larger number of available codes and, more importantly, in a lower P_{error} for the same number of simultaneous users. For a fixed N, increasing w potentially increases the SIR and hence reduces

Table 1. Maximum Number of Codes and Original *m* Codes for the Different Cases Used in the Performance Analysis Given in Subsection 3.B

N	w	m	Max. No. of Codes	Original m Codes
12	3	3	14	c_1 = [0,0,0,4,0,0,7,0,9,0,0,0]
				c_2 = [0,2,0,0,0,6,0,0,0,10,0,0]
				c_3 = [0,0,3,0,5,0,0,0,0,0,0,12]
15	3	3	22	c_1 = [0,0,0,0,0,6,0,0,9,10,0,0,0,0,0]
				c_2 = [1,2,0,0,0,0,0,0,0,0,0,13,0,0]
				c_3 = [0,0,0,0,5,0,7,0,0,0,0,12,0,0,0]
21	3	6	59	c_1 = [0,0,0,0,5,6,0,0,0,0,0,12,0,0,0,0,0,0,0,0,0]
				c_2 = [0,0,3,0,0,0,7,0,0,0,0,0,0,0,15,0,0,0,0,0,0]
				c_3 = [1,0,0,4,0,0,0,0,0,0,0,0,0,0,14,0,0,0,0,0,0]
				c_4 = [0,0,0,0,0,0,0,8,0,10,0,0,13,0,0,0,0,0,0,0,0]
				c_5 = [0,0,0,0,0,0,0,0,0,9,0,0,0,0,0,0,0,0,0,18,0,20,0]
				c_6 = [0,2,0,0,0,0,0,0,0,0,0,0,0,0,0,0,0,17,0,0,0,21]

P_{error}; however, it will be more difficult to obtain the maximum number of original $\tilde{m}$ codes, since the restrictions imposed greatly reduce the number of available codes for selection. We also considered the case in which ($N = 21$, $w = 3$, $m = 6$) and found that the system could support $K = 48$ users at $P_{\text{error}} = 10^{-9}$ (the original m codes are also given in Table 1). Finally, for the same N and w, the maximum number of available codes and their performance are comparable with, if not better than, previously proposed codes for wavelength-encoding/temporal-spreading OCDMA systems.[8,18]

Again we note that the above results are only approximate and are based on a first-order analysis. In real systems the encoded and the decoded signals will depend on the temporal reflection and the spectral responses of the CMG's and, in general, are not rectangular (see Figs. 4 and 5). The nonideal spectral slices can increase multiuser interference in the form of cross talk, thereby decreasing the SIR. Also, in a purely asynchronous system, perfect slot synchronization among the different users is not maintained. Thus the cross-correlation peaks will decrease, because of imperfect temporal overlap of the pulses, and in this case the variance of multiuser interference will be less than for a slot synchronous case.[6] Finally, as with most other publications in this field, we calculated the SIR, using average variances for multiuser interference [Eq. (3)]. In fact, the variance depends on the sequence pairs under consideration and, in extreme cases, the corresponding performance can be far from average. A more accurate estimation of P_{error} would involve a Monte Carlo simulation; however, that is beyond the scope of the present analysis.

4. Discussion

In this section we discuss the various practical aspects that are relevant to our proposed system.

A. Fabrication of Specially Designed Chirped Moiré Gratings

The first practical aspect we consider is the realization and fabrication of CMG's with specially designed spectral characteristics (i.e., the ability to suppress selected stop bands). Previously, CMG's were difficult to fabricate with good performance characteristics; however, the numerous advances in grating fabrication technology should help us overcome this problem. In fact the technique of fabricating CMG's with dual exposure of a single linearly chirped phase mask has yielded good results.[11] We adopted this technique and included the use of amplitude masks in the exposure processes to tailor the spectral characteristics of the CMG's and obtained excellent agreement between measured and simulated results.[15] Furthermore, there have been recent reports on the fabrication of very long (1-m-long) CMG structures by use of the scanning-fiber/phase-mask technique.[19] These experimental successes show the feasibility of obtaining CMG's with good performance characteristics. Finally, we note that for an individual user bit rate at the optical carrier standard of OC-3 (OC-12) of 155.52 Mbit/s (622.08 Mbit/s) the corresponding bit window is $\approx$6.43 ns (1.61 ns). To encode a signal so that it occupies this time requires a CMG approximately 67 cm (17 cm) long, assuming a fiber index of 1.45—well within the available technology.

B. Chromatic Fiber Dispersion

The second issue deals with chromatic fiber dispersion (CFD). Without proper compensation CFD is known to be a detrimental problem in optical communication systems that require long distances of propagation or high speeds of operation (which require the use of short optical pulses). CFD can also be a significant problem in OCDMA systems that use broadband sources, especially those based on phase encoding of ultrashort optical pulses.[20] These systems distinguish properly and improperly decoded signals on the basis of whether or not the ultrashort optical input pulse is fully reconstructed or remains a pseudorandom noise burst. In this type of OCDMA system, the phases of all wavelength components must be accounted for and the effects of CFD must be included. Otherwise, if CFD is not compensated, the ultrashort pulses cannot be reconstructed properly.

Our proposed system does not require the use of coherent pulses, and even if they were used, we are not attempting to reconstruct the pulses (the fact that we perform spectral slicing and not phase encoding precludes this). For our system CFD becomes problematic only if it significantly spreads the spectral slices in time so that the decoder CMG cannot recover them all into the same time slot. Typical local area networks are less than 2 km in length. As an example, a dispersion of 17 ps/(nm · km) for standard fiber results in a time spread of 340 ps after propagation for a 10-nm-wide signal. If the duration of the time slots is longer than 340 ps, then the wavelengths of a properly decoded signal will still be recovered into the same time slot. Thus the use of longer CMG's can give longer time slots so that the system is more tolerant to the effects of CFD. Of course, requiring a time slot to accommodate the effects of CFD will place a limit on the individual user bit rate, since for a fixed code length N (corresponding to N time slots) increasing their duration decreases the user bit rate. For an individual bit rate at the OC-3 standard, using a time slot of 400 ps to account for CFD would give a code length $N = 16$. This system supports approximately 20 users for an aggregate data rate of >3 Gbit/s. Finally, we can minimize the effects of CFD by either using dispersion-shifted fiber or operating near the zero-dispersion wavelength $\lambda = 1300$ nm.

C. Time Gating

Time gating is used to select the time slot within the bit window when the detector samples the decoded signal. It is not a necessary requirement, since we can always integrate the detected optical power over the entire bit window. However, as multiuser interference increases, primarily outside the desired time

slot, incorporating a time gate within the detection unit significantly increases the performance of the system, especially if a fixed threshold detector is used. This improvement results from isolating the time slot in which all the energy of the properly decoded signal resides so that the only multiuser interference arises from the nonideal or nonrectangular spectral characteristics of the CMG encoders–decoders (see Fig. 4).

Time gating can be performed electronically. With currently available technology this requires the duration of the time slot to be ≈500 ps long. Given that the time slot needs to be at least 340 ps long to accommodate CFD for a 10-nm-wide signal in a 2-km link over standard fiber, the use of electronic time gating does not significantly change the individual user bit rates nor the overall system capacity.

D. Other Factors

Although in our discussions we assumed that the N reflection stop bands span the entire BW of the input pulse, $[\lambda_{\min}, \lambda_{\max}] = [\lambda_{\min}^{\text{pulse}}, \lambda_{\max}^{\text{pulse}}]$, we can easily extend our analysis to the case in which the pulse BW is larger than the CMG spectral response, $[\lambda_{\min}, \lambda_{\max}] \subset [\lambda_{\min}^{\text{pulse}}, \lambda_{\max}^{\text{pulse}}]$. In this case the number of wavelengths to be used for wavelength encoding is limited only by the pulse BW. Furthermore, a larger number of codes can be obtained for the same values of N and w—not only can we define more original m codes; we also have a larger wavelength range in which to wavelength shift them (in this case the maximum number of original codes $\tilde{m} \neq \lfloor N/w \rfloor$). However, the amount of CFD depends on the BW of the broadband source and/or the CMG's. Although a broader BW potentially allows for more codes to be defined, it comes at the expense of additional CFD.

We also considered only a linear detection system. An alternative detection scheme, which may be more useful especially for asynchronous transmission or coherent systems, is one in which a nonlinear optical detector is used that distinguishes signals based on peak intensity and/or duration rather than on average energy.[21]

5. Summary

In summary, we have proposed an OCDMA system that uses CMG's for encoding and decoding. The use of CMG's is a special case of using optical filters (including in-fiber Bragg gratings) as a means of implementing wavelength-encoding OCDMA. They also provide an additional degree of freedom by allowing for simultaneous encoding in the time domain, which is a significant advantage for encoding. We have presented the designs of one-coincidence codes that take into account the linear wavelength–time relationship of the CMG's that are used for encoding and decoding. Although the linear wavelength–time relationship of the CMG's places restrictions on code design (the two-dimensional nature of encoding in both wavelength and time domains is not fully exploited), the maximum number of available codes and their performance are comparable with previously proposed ones (of the same length). More importantly, the fabrication of specially designed CMG's is reasonably straightforward, and our implementation is simple, requiring only passive components for performing all the encoding and decoding operations in fiber.

The authors thank the reviewers of the initial version of this paper for their constructive comments. This study was supported in part by grants from the Natural Sciences and Engineering Research Council of Canada (NSERC) and Photonics Research Ontario. L. R. Chen acknowledges the NSERC and the Walter C. Sumner Foundation for financial support. The authors thank F. R. Kschischang (University of Toronto) and S. LaRochelle (Université Laval) for fruitful discussions. This paper was presented in part as a poster at the Optical Society of America Annual Meeting, Baltimore, Maryland, 4–9 October 1998.

References and Notes

1. N. Karafolas and D. Uttamchandani, "Optical fiber code division multiple access networks: a review," Opt. Fiber Technol. **2,** 149–168 (1996).
2. D. D. Sampson, G. J. Pendock, and R. A. Griffin, "Photonic code-division multiple-access communications," Fiber Integr. Opt. **16,** 129–157 (1997).
3. L. R. Chen, S. D. Benjamin, P. W. E. Smith, J. E. Sipe, and S. Juma, "Ultrashort pulse propagation in multiple-grating fiber structures," Opt. Lett. **22,** 402–404 (1997).
4. L. R. Chen, S. D. Benjamin, P. W. E. Smith, and J. E. Sipe, "Applications of ultrashort pulse propagation in Bragg gratings for wavelength-division-multiplexing and code-division multiple access," J. Quantum Electron. **34,** 2117–2129 (1998).
5. S. Wang, H. Erlig, H. R. Fetterman, and J. Feinberg, "One-dimensional photonic crystals for CDMA," in *Multimedia Networks: Security, Displays, Terminals, and Gateways*, V. Bove, B. Derryberry, C. R. Holliday, L. S. Lome, V. Markandey, A. G. Teschev, and B. Vasudev, eds., Proc. SPIE **3228,** 408–417 (1997).
6. H. Fathallah, L. A. Rusch, and S. LaRochelle, "Passive optical fast frequency-hop CDMA communications system," J. Lightwave Technol. **17,** 397–405 (1999).
7. H. Geiger, A. Fu, P. Petropoulos, M. Ibsen, D. J. Richardson, and R. I. Laming, "Demonstration of a simple CDMA transmitter and receiver using sampled fiber gratings," in *Proceedings of the 24th European Conference on Optical Communications* (*ECOC'98*) (Institute of Electrical and Electronics Engineers, Piscataway, N.J., 1998), Vol. 1, pp. 337–338.
8. L. Tančevski and I. Andonovic, "Wavelength-hopping/time-spreading code-division multiple-access systems," Electron. Lett. **30,** 1388–1390 (1994).
9. G. E. Town, K. Sugden, J. A. R. Williams, I. Bennion, and S. B. Poole, "Wide-band Fabry–Pérot-like filters in optical fiber," Photonics Technol. Lett. **7,** 78–80 (1995).
10. C. Martijn de Sterke, J. N. Bright, P. A. Krug, and T. E. Hammon, "Observation of an optical Wannier–Stark ladder," Phys. Rev. E **57,** 2365–2370 (1998).
11. L. A. Everall, K. Sugden, J. A. R. Williams, I. Bennion, X. Liu, J. S. Aitchison, and R. M. De La Rue, "Fabrication of multipassband moiré resonators in fibers by dual-phase-mask exposure method," Opt. Lett. **22,** 1473–1475 (1997).
12. L. Poladian, "Group delay reconstruction for fiber Bragg gratings in reflection and transmission," Opt. Lett. **22,** 1571–1573 (1997).
13. D. Taverner, D. J. Richardson, M. N. Zervas, L. Reekie, L.

Dong, and J. L. Cruz, "Investigation of fiber grating-based performance limits in pulse stretching and recompression schemes using bidirectional reflection from a linearly chirped fiber grating," Photonics Technol. Lett. **7,** 1436–1438 (1995).
14. L. R. Chen, D. J. F. Cooper, and P. W. E. Smith, "Transmission filters with multiple flattened passbands based on chirped Moiré gratings," Photonics Technol. Lett. **10,** 1283–1285 (1998).
15. L. R. Chen, H. S. Loka, D. J. F. Cooper, P. W. E. Smith, R. Tam, and X. Gu, "Fabrication of transmission filters with single or multiple flattened passbands based on chirped Moiré gratings," Electron. Lett. **35,** 584–585 (1999).
16. The notation $(m|n)$ represents the number of ways of selecting n objects from a set of m objects regardless of order and is defined as $(m|n) = [m!/n!(m - n)!]$.
17. A. A. Shaar and P. A. Davies, "A survey of one-coincidence sequences for frequency-hopped spread-spectrum systems," IEE Proc. F **131,** 719–724 (1984).
18. E. Jugl, T. Kuhwald, and K. Iversen, "Algorithm for construction of (0,1)-matrix codes," Electron. Lett. **33,** 227–229 (1997).
19. M. Ibsen, M. K. Durkin, R. I. Laming, "Chirped moiré fiber gratings operating on two-wavelength channels for use as dual-channel dispersion compensators," Photonics Technol. Lett. **10,** 84–86 (1998).
20. H. P. Sardesai, C.-C. Chang, and A. M. Weiner, "A femtosecond code-division multiple-access communication system test bed," J. Lightwave Technol. **16,** 1953–1964 (1998).
21. Z. Zheng, A. M. Weiner, J. H. Marsh, and M. M. Karkhanehchi, "Ultrafast optical thresholding based on two-photon absorption GaAs waveguide photodetectors," Photonics Technol. Lett. **9,** 493–495 (1997).